Twolevel quantum systems: States, phases, and holonomy

H. Urbantke

Citation: Am. J. Phys. **59**, 503 (1991); doi: 10.1119/1.16809
View online: http://dx.doi.org/10.1119/1.16809
View Table of Contents: http://ajp.aapt.org/resource/1/AJPIAS/v59/i6
Published by the American Association of Physics Teachers

Two-level quantum systems: States, phases, and holonomy

H. Urbantke
Institut für Theoretische Physik, Universität Wien, Boltzmanngasse 5, A-1090 Wien, Austria

(Received 27 April 1990; accepted for publication 13 September 1990)

For a two-level quantum mechanical system, pictorial descriptions of states, state vectors, phases, and their time evolution on the two- and three-sphere are discussed, including adiabatic changes and Berry's phase.

I. INTRODUCTION

The standard formulation of quantum mechanics uses complex Hilbert space and thus complex numbers in an essential way. Of course, it would be possible to do with real numbers alone, but then the formalism would "cry for complex numbers." We do not want to speculate here on the possible origin of the occurrence of complex numbers in quantum physics, but rather address the *difficulty* of *illustrating* and *visualizing complex vector spaces* even in the finite-dimensional case, i.e., the case of N-level systems. For a two-level system, the Hilbert space is complex two-dimensional = real four-dimensional and thus beyond immediate visualization: Complex superposition is not easy to illustrate! However, due to the fact that only normalized vectors matter, the dimension is reduced by one, which brings us into the domain of visualizability, although the advantages of linearity of the space are lost.

Since many features of quantum mechanics can already be discussed using two-level systems,[1] it seems worthwhile to put together several aspects of geometric visualizations that are possible here, some well known and some less well known but of recent interest.

II. PURE AND MIXED STATES

Almost every textbook on quantum mechanics—let us quote only one of them[2] for more detailed reference—introduces the concept of pure and mixed states and illustrates it with the help of two-level systems. Here, the Hilbert space $\mathbf{H}$ can be taken as the space $\mathbf{C}^2$ of pairs $|z\rangle = (z_1,z_2)$ of complex numbers, equipped with the scalar product (an overbar denotes complex conjugation)

$$\langle z|w\rangle := \bar{z}_1 w_1 + \bar{z}_2 w_2. \tag{1}$$

The elements of $\mathbf{H} = \mathbf{C}^2$ are the *state vectors*. They determine *pure states*. A pure state is formally given as the set of complex nonzero multiples $\lambda|z\rangle$ of a nonzero state vector $|z\rangle$ ("vector ray"), or the set of multiples $\lambda|z\rangle$, where λ and $|z\rangle$ are restricted by $|\lambda| = 1$ and $\langle z|z\rangle = 1$ ("unitary ray")—the well-known normalization condition that is preserved by quantum mechanical time evolution. The same information is also contained in the projection operator

$$\rho := |z\rangle\langle z| \tag{2}$$

or, in matrix form,

$$\rho_{ik} = z_i\bar{z}_k, \quad (\rho_{ik}) = \begin{pmatrix} z_1\bar{z}_1 & z_1\bar{z}_2 \\ z_2\bar{z}_1 & z_2\bar{z}_2 \end{pmatrix}, \tag{3}$$

where $|z\rangle$ is assumed normalized; a phase factor λ ($|\lambda|^2 = 1$) multiplying $|z\rangle$ obviously drops out from ρ. Thus state vectors, even when normalized, contain more mathematical information than states (rays, projection operators).

The matrix ρ_{ik}—called the *density matrix* of the pure state—enjoys the properties of Hermiticity, normalization, and positivity

$$\rho^\dagger = \rho,$$

$$\operatorname{tr}\rho := \sum_i \rho_{ii} = 1,$$

$$\langle w|\rho|w\rangle := \sum_{i,k} \bar{w}_i \rho_{ik} w_k = |\langle w|z\rangle|^2 \geqslant 0 \tag{4}$$

for all $|w\rangle$; further, we have the projection property

$$\rho^2 = \rho. \tag{5}$$

The density matrix description has the advantage of generalizing to the concept of *mixed state*; formally, the density matrix of a mixed state is characterized by the properties (4), while the projection property (5) is dropped. Density matrices of mixed states are obtained by taking linear combinations $\Sigma r_A \rho_A$ of density matrixes ρ_A of pure states with real positive coefficients r_A summing to unity, $\Sigma r_A = 1$. The set of all density matrices is then closed under taking such combinations: It is a convex set (in the real affine space of all Hermitian matrices of unit trace). We do not go into the statistical significance of these features, which are quite general, but turn to the visualization in the $\mathbf{C}^2$, i.e., two-level, case.

The set of 2×2 Hermitian matrices is a four-dimensional real vector space; the condition of unit trace reduces to a three-dimensional submanifold (an affine hyperplane with $\frac{1}{2}$ times the unit matrix as a distinguished origin), in which we have to locate the domain of positivity. One way of doing this is to write the real quantities ρ_{11}, ρ_{22} with $\rho_{11} + \rho_{22} = 1$ as

$$\rho_{11} = \tfrac{1}{2}(1 + R_3), \quad \rho_{22} = \tfrac{1}{2}(1 - R_3) \tag{6a}$$

and the complex quantity $\rho_{21} = \overline{\rho_{12}}$ as

$$\rho_{21} = \tfrac{1}{2}(R_1 + iR_2), \tag{6b}$$

thus introducing a formal vector $\mathbf{R} = (R_1,R_2,R_3) \in \mathbf{R}^3$. This parametrization will also be written as

$$\rho\tfrac{1}{2}(\mathbf{1} + \mathbf{R}\cdot\boldsymbol{\sigma}), \tag{6c}$$

where $\mathbf{1}$ is the 2×2 unit matrix and $\boldsymbol{\sigma} = (\sigma_1,\sigma_2,\sigma_3)$ are the Pauli matrices. One point of this vectorial way of writing ρ is that *if* the two-level system corresponds to a spin-1/2 particle with translational degrees of freedom neglected, then $\mathbf{R}$ is proportional to the expectation value of the spin of the particle in the state ρ and thus is a vector in our *ordinary* three-space; otherwise, the $\mathbf{R}^3$ introduced here is auxiliary and *formal*.

Now putting $w_2 = 0$; $w_1 = 0$; $w_1:w_2 = -\rho_{12}:\rho_{11}$ in the positivity condition we find $\rho_{11} \geqslant 0$; $\rho_{22} \geqslant 0$; $\rho_{11}\rho_{22} - \rho_{12}\rho_{21} \geqslant 0$, or, in terms of $\mathbf{R}$,

$$1 - \mathbf{R}^2 \geqslant 0. \tag{7}$$

This condition also checks to be sufficient for positivity and

shows that in our auxiliary $\mathbf{R}^3$ the domain of positivity is just the closed unit ball, which is obviously a convex set. The condition $\rho^2 = \rho$ for pure states is equivalent, in $\mathbf{R}$ language, to

$$\mathbf{R}^2 = 1, \tag{8}$$

illustrating the general fact that the pure states form the extremal points of the convex set: Here, they form the surface $\mathbf{S}^2$ (= unit sphere) of the unit ball.

In what follows we shall concentrate mainly on pure states and on the *visualization of the phases* of the corresponding normalized *state vectors*, in the $\mathbf{S}^2$ picture just obtained as well as in another picture that we introduce right now.

III. PURE STATES AND STATE VECTORS

A. (Stereographic) $\mathbf{S}^3$ picture

Consider the Hilbert space $\mathbf{C}^2$ as a real vector space $\mathbf{R}^4$: the components of $|z\rangle$ then are

$$X := (\mathrm{Re}\, z_1 =: X_1, \mathrm{Im}\, z_1 =: X_2, \mathrm{Re}\, z_2 =: X_3, \mathrm{Im}\, z_2 =: X_4), \tag{9}$$

and the condition of normalization is

$$1 = |z_1|^2 + |z_2|^2 = X_1^2 + X_2^2 + X_3^2 + X_4^2. \tag{10}$$

This is the equation of the unit sphere $\mathbf{S}^3 \subset \mathbf{R}^4$. Although only three-dimensional, $\mathbf{S}^3$ is already hard to imagine in its entirety, and is known to have some surprising topological properties. Consider normalized state vectors corresponding to the same pure state

$$(\rho_{ik}) = (z_i \bar{z}_k) = \tfrac{1}{2}(1 + \mathbf{R}\cdot\boldsymbol{\sigma}). \tag{11}$$

They are obtained from one of them, (z_1, z_2), by multiplying by an arbitrary phase factor $\lambda = e^{i\alpha}$,

$$z_k \to e^{i\alpha} z_k = z_k(\alpha), \tag{12}$$

where α is real. What does the corresponding point on $\mathbf{S}^3$ do as we vary α?

Separating real and imaginary parts, we obtain

$$X \to \cos\alpha X + \sin\alpha JX = X(\alpha),$$
$$JX := (-X_2, X_1, -X_4, X_3), \tag{13}$$

a normalized combination of two orthogonal unit vectors of $\mathbf{R}^4$ for every α: The point thus traces a *great circle* on $\mathbf{S}^3$, and this circle represents the state. Repeating this for all pure states gives the *Hopf fibering* of $\mathbf{S}^3$ by a system of circles (*Clifford parallels*) which themselves can be represented by points of a sphere $\mathbf{S}^2$, as we saw above.

One way of visualizing this fibering is to use a stereographic map of $\mathbf{S}^3$ onto an "equatorial" hyperplane $\mathbf{R}^3$, in complete analogy to the well-known stereographic map of $\mathbf{S}^2$ onto $\mathbf{R}^2$. We shall perform our stereographic projection onto the equatorial hyperplane given by $X_4 = 0$: This will leave us with some convenient axial symmetry. The stereographic maps send circles to circles; but while the original fibering is by circles of the same radius (= 1), the image circles will not all have the same radii. Rather, image circles of the same radius r form a torus $\mathbf{T}^2(r) \subset \mathbf{R}^3$, and by varying r one arrives at a coaxial concentric system of nested tori, all orthogonal to a fixed concentric sphere. On each of these tori, the circles are *not* meridional but are known as *Villarceau* circles, each contained in a plane that touches the torus at just *two* points (Fig. 1).[3]

It is not hard to verify the statements made. Let (x_1, x_2, x_3) be the Cartesian coordinates in the equatorial

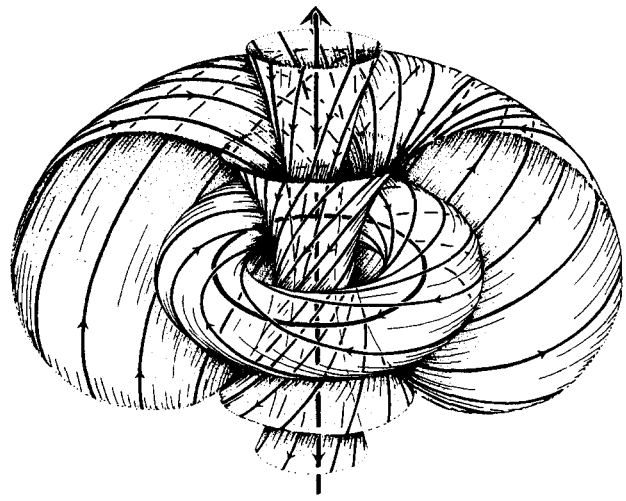

Fig. 1. Stereographic map of the Hopf fibering by Clifford parallels as drawn by Penrose[3] (courtesy Cambridge U.P.).

$\mathbf{R}^3 \subset \mathbf{R}^4$ given by $X_4 = 0$ onto which the stereographic projection is made. If we project from $(0,0,0,\pm 1)$, the running point (X_1, X_2, X_3, X_4) on $\mathbf{S}^3$ is related to its stereographic image (x_1, x_2, x_3) by (see Fig. 2)

$$X_4 = \pm(\mathbf{x}^2 - 1)/(\mathbf{x}^2 + 1),$$
$$X_i = 2x_i/(\mathbf{x}^2 + 1) \quad (i = 1,2,3),$$
$$\mathbf{x}^2 := x_1^2 + x_2^2 + x_3^2. \tag{14}$$

Exploiting the normalization of $|z\rangle$ and separating an absolute phase from the relative phase φ between z_1 and z_2 we now write

$$z_1 = \cos(\vartheta/2) e^{i\varphi_1} \equiv \cos(\vartheta/2) e^{-i\varphi/2} e^{i(\varphi_1 + \varphi_2)/2},$$
$$\varphi := \varphi_2 - \varphi_1, \tag{15}$$
$$z_2 = \sin(\vartheta/2) e^{i\varphi_2} \equiv \sin(\vartheta/2) e^{i\varphi/2} e^{i(\varphi_1 + \varphi_2)/2},$$

thus defining an angle ϑ, $0 \leqslant \vartheta \leqslant \pi$. Varying α will only change the absolute phase $(\varphi_1 + \varphi_2)/2$ but neither φ nor ϑ. The latter appear in $\mathbf{R}$ as [cf. (3) and (6)]

$$R_3 = \cos\vartheta, \quad R_1 + iR_2 = \sin\vartheta e^{i\varphi}, \tag{16}$$

representing the usual polar angles in the $\mathbf{S}^2$ picture of pure states. [Also note that R_1, R_2, R_3 are related to Re z, Im z, where $z := z_2/z_1 = \tan(\vartheta/2)e^{i\varphi}$, by a stereographic relation similar to (14)!]

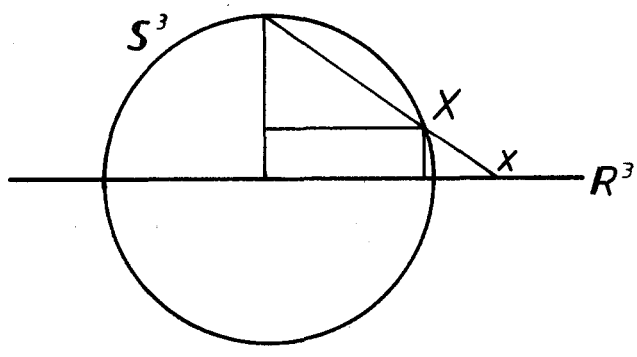

Fig. 2. Stereographic projection of $\mathbf{S}^3$ onto its equatorial hyperplane $\mathbf{R}^3$. From similar triangles and the normalization condition one obtains Eqs. (14).

Observe now, first, that the points of the circle on S^3 traced by the initial point $(z_1,z_2) = (X_1,X_2,X_3,X_4)$ all have $|z_1(\alpha)|^2 = X_1^2(\alpha) + X_2^2(\alpha) = \cos^2\vartheta/2$. It follows from (14) that their stereographic projections have

$$4(x_1^2 + x_2^2)/(\mathbf{x}^2 + 1)^2 = \cos^2(\vartheta/2). \tag{17}$$

The set of all points $\mathbf{x}\in\mathbf{R}^3$ satisfying this equation forms a surface of revolution, obtained by rotating the curve in the (1,3)-plane given by

$$2x_1/(x_1^2 + x_3^2 + 1) = \cos(\vartheta/2) \tag{18}$$

around the three-axis. Excepting the limiting cases $\vartheta = 0$, π, this curve is a circle of radius $\tan\vartheta/2$, with center on the one-axis a distance $1/\cos(\vartheta/2)$ from the origin, and thus orthogonal to the unit circle $x_1^2 + x_3^2 = 1$ ($1/\cos^2(\vartheta/2) - \tan^2(\vartheta/2) \equiv 1$!). It follows that the surface of revolution is a torus orthogonal to the unit sphere $\mathbf{x}^2 = 1$. This gives us the picture of a family of nested, coaxial, concentric tori, parametrized by ϑ in the interval $0 < \vartheta < \pi$, plus the degenerate forms as $\vartheta \to 0$ or $\vartheta \to \pi$ [Fig. 3(a)].

Observe now, second, that the points of the circle on S^3 also have

$$\sin(\vartheta/2)e^{i\varphi}z_1(\alpha) - \cos(\vartheta/2)z_2(\alpha) = 0. \tag{19}$$

Taking the real part and performing the stereographic substitution (14), we obtain

$$x_3 = \tan(\vartheta/2)(\cos\varphi\, x_1 - \sin\varphi\, x_2). \tag{20}$$

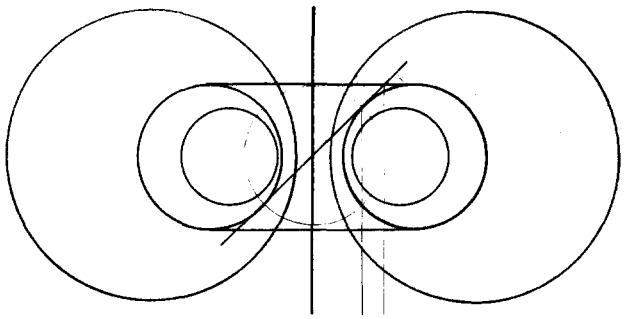

(a)

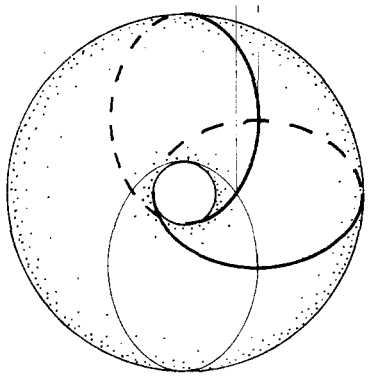

(b)

Fig. 3. (a) Meridional section through a family of nested coaxial concentric tori orthogonal to the unit sphere $S^2 \subset \mathbf{R}^3$. For one torus, a doubly tangent plane orthogonal to the plane of our section is indicated; (b) Top view of a torus as intersected by a doubly tangent plane along a pair of Villarceau circles intersecting at the points of tangency. One of them has also been rotated about 90° to show the linkage. (In this view, the circles appear as ellipses with one focus at the center of the figure.)

The set of all $\mathbf{x}\in\mathbf{R}^3$ satisfying this equation is a plane through the origin whose angle of inclination against the (1,2)-plane is $\vartheta/2$; varying φ will rotate the plane around the three-axis. Consideration of the position $\varphi = 0$ makes it clear that the plane touches the torus above at two points $[\sin(\vartheta/2) \equiv \tan(\vartheta/2) : 1/\cos(\vartheta/2)]$ [Fig. 3(a)]. Its complete intersection with the torus *contains* the stereographic image of our circle on S^3—in fact, it *consists* of the stereographic images obtained by projection from both, (0,0,0,1) *and* (0,0,0, -1), since the sign dichotomy introduced in (14) does not show up in (17) and (20).

Finally, performing the stereographic substitution in the imaginary part of (19) gives

$$\mathbf{x}^2 \mp 2\tan(\vartheta/2)(\sin\varphi\, x_1 + \cos\varphi\, x_2) = 1, \tag{21}$$

the equations of two spheres of radius $1/\cos(\vartheta/2)$ with centers on the line of intersection of (20) and $x_3 = 0$ at distance $\pm\tan(\vartheta/2)$ from the origin. Intersecting the plane (20) with these spheres gives the image circles under the $\pm$ projections, of radius $r = 1/\cos(\vartheta/2)$ [Fig. 3(b)].

Deciding on one of the projections and gradually varying φ now shows that all image circles on the same torus are *linked*; the nestedness of the tori for different values of ϑ shows the linkage of any two image circles.

An advantage of this picture is to show some features of the topological situation; in particular, how each circle links all the others. However, the S^2 nature of the quotient of S^3 by the fibering is not seen directly: States whose phase circles in the stereographic projection are on the same torus correspond, in the S^2 picture, to points of a circle of constant latitude [cf. Eq. (16)]—but the occurrence of the degenerate tori ($\vartheta = 0$ or π) prevents one from reading off the topology of the state space from the stereographic S^3 picture immediately.

B. The S^2 picture

We therefore turn to another visualization of normalized state vectors which is directly based on the S^2 description of pure states given above. We do not explain its relation to the homomorphism of the unimodular unitary group SU(2) onto the group of rotations in real Euclidean $\mathbf{R}^3$, SO(3,**R**) (see, e.g., Ref. 4), nor its immediate derivation from **R**. Penrose's Lorentz-covariant "null flag" representation of two-component spinors,[5] but simply parachute onto the elementary formulas allowing the visualization.

Thus, in addition to the unit vector **R** associated with the density matrix of a pure state, which in this case is [cf. (3) and (6)]

$$\begin{aligned}\mathbf{R} &= (2\,\mathrm{Re}\,\rho_{21}, 2\,\mathrm{Im}\,\rho_{21}, \rho_{11} - \rho_{22}) \\ &= [z_1\bar{z}_2 + z_2\bar{z}_1, i(z_1\bar{z}_2 - z_2\bar{z}_1), |z_1|^2 - |z_2|^2,\end{aligned} \tag{22}$$

we define two more vectors **P**, **Q** from $\mathbf{R}^3$ by

$$\mathbf{P} + i\mathbf{Q} = \mathbf{Z} := (z_1^2 - z_2^2, i(z_1^2 + z_2^2), -2z_1z_2). \tag{23}$$

Using $\langle z|z\rangle = 1$, one easily verifies that, in addition to $\mathbf{R}^2 = 1$, we have

$$\mathbf{Z}^2 = 0, \quad \mathbf{R}\cdot\mathbf{Z} = 0, \quad \mathbf{Z}\cdot\mathbf{Z} = 2, \quad \mathbf{Z}\times\bar{\mathbf{Z}} = -2i\mathbf{R}, \tag{24}$$

from which

$$\mathbf{P}^2 = \mathbf{Q}^2 = 1, \quad \mathbf{P}\cdot\mathbf{Q} = \mathbf{R}\cdot\mathbf{P} = \mathbf{R}\cdot\mathbf{Q} = 0, \quad \mathbf{P}\times\mathbf{Q} = \mathbf{R}. \tag{25}$$

These relations show that **P**, **Q**, **R**, in that order, form a positively oriented orthonormal triad. Since we have interpreted **R** as the position vector of a point on the unit sphere

$\mathbf{S}^2 \subset \mathbf{R}^3$, we can visualize $\mathbf{P}$ as a unit tangent vector to $\mathbf{S}^2$ at $\mathbf{R}$ (and $\mathbf{Q}$ as well, but because of orthonormality and orientation, it does not contain new information over and above $\mathbf{R}$, $\mathbf{P}$). The essential observation is now that, while $\mathbf{R}$ is independent of any phase change in $|z\rangle$, $\mathbf{P}$ is sensitive to such a change: If $|z\rangle \to e^{i\alpha}|z\rangle$, then $\mathbf{Z} \to e^{2i\alpha}\mathbf{Z}$ and thus

$$\mathbf{P} \to \cos 2\alpha \mathbf{P} - \sin 2\alpha \mathbf{Q} = \mathbf{P}(\alpha), \tag{26}$$

i.e., $\mathbf{P}$ gets rotated in the tangent plane to $\mathbf{S}^2$ at $\mathbf{R}$ by the amount 2α. Note that $\mathbf{P}$ registers phase changes mod π only: $|z\rangle$ and $-|z\rangle$ still give the same $\mathbf{P}$, and $\mathbf{R}$, $\mathbf{P}$ together determine $|z\rangle$ up to sign. This, then, is the second visualization of normalized state vectors. The $\mathbf{S}^3$ nature of their totality is now not immediately apparent (Fig. 4).

It is tempting to interpret the basic algebraic operations available in $\mathbf{C}^2$ in this picture, and to a certain extent this can indeed be done—the limitations coming from the sign ambiguity just mentioned. For instance, an interpretation of the basic scalar product (probability amplitude) $\langle z|z'\rangle$ of two normalized state vectors is as follows.

Consider first the probability $|\langle z|z'\rangle|^2$, which is independent of the phases of $|z\rangle$, $|z'\rangle$ and therefore should be interpretable in terms of the corresponding $\mathbf{R}$, $\mathbf{R}'$ alone. Indeed, one checks that $|\langle z|z'\rangle|^2$ equals the squared distance from the origin of the chord from $\mathbf{R}$ to $\mathbf{R}'$, or that

$$\sqrt{1 - |\langle z|z'\rangle|^2} = \tfrac{1}{2}|\mathbf{R} - \mathbf{R}'|. \tag{27}$$

Thus, in particular, if $|z\rangle$, $|z'\rangle$ are orthogonal, the chord is a diameter of $\mathbf{S}^2$.

For further elaboration, it is of advantage to consider also the bilinear antisymmetric quantity

$$\{z|w\} := z_1 w_2 - z_2 w_1, \tag{28}$$

which satisfies

$$|\{z|w\}|^2 + |\langle z|w\rangle|^2 \equiv \langle z|z\rangle\langle w|w\rangle. \tag{29}$$

(If $|z\rangle$ and $|w\rangle$ are normalized spin-1/2 state vectors, then $\{z|w\}/\sqrt{2}$ is just the probability amplitude for finding total spin 0 in the two-particle state $|z\rangle \otimes |w\rangle$; and $|\{z|w\}| = \frac{1}{2}|\mathbf{R} - \mathbf{R}'|$.)

It is less easy to verify that the phase angle $\arg\langle z|z'\rangle$ is given by the following prescription. Draw the oriented great circle on $\mathbf{S}^2$ which leads from $\mathbf{R}$ to $\mathbf{R}'$ (we assume $\langle z|z'\rangle \neq 0$ so that $\mathbf{R}$, $\mathbf{R}'$ are not antipodes and this circle is unique). Call β, β' the angles that $\mathbf{P}$, $\mathbf{P}'$ make with this circle in the sense of its orientation. Then

$$\begin{aligned} 2\arg\langle z|z'\rangle &= \beta' - \beta, \\ 2\arg\{z|z'\} &= \beta' + \beta, \end{aligned} \tag{30}$$

the latter actually being independent of which circle on $\mathbf{S}^2$ we draw from $\mathbf{R}$ to $\mathbf{R}'$: It need not be the great circle.

Finally, we consider a complex linear superposition

$$|z\rangle = N(a'|z'\rangle + a''|z''\rangle) \tag{31}$$

of nonproportional normalized state vectors, where $N > 0$ is chosen to normalize $|z\rangle$. Let then $|z'\rangle; |z''\rangle$ be represented by $\mathbf{R}'$, $\mathbf{P}'$; $\mathbf{R}''$, $\mathbf{P}''$ on $\mathbf{S}^2$, and ask for $\mathbf{R}$, $\mathbf{P}$ representing $|z\rangle$. First change the phases of $|z'\rangle, |z''\rangle$ appropriately to swallow the phases of a', a'': After the corresponding rotations of $\mathbf{P}'$, $\mathbf{P}''$, we may thus assume a', a'' to be real. Next look at $\{z|z'\}$ and $\{z|z''\}$ and their interpretation to arrive at the following prescription for $\mathbf{R}$, $\mathbf{P}$. Find the oriented circle on $\mathbf{S}^2$ that leads from $\mathbf{R}'$ to $\mathbf{R}''$ and makes the same angle with $\mathbf{P}'$ and $\mathbf{P}''$ (positions after the rotations just mentioned; this will not be a great circle, in general). Then $\mathbf{R}$ will also be on this circle and $\mathbf{P}$ will make the same angle with it. To locate $\mathbf{R}$ on it, intersect it with the "Apollonian" sphere, which is the set of points in $\mathbf{R}^3$ whose distances from $\mathbf{R}'$ and from $\mathbf{R}''$ are in the ratio $|a''|:|a'|$. There are two intersection points and thus two candidates for $\mathbf{R}$, because on the one hand $-|z''\rangle$ is represented by $\mathbf{R}''$, $\mathbf{P}''$ as well as $|z''\rangle$ is, while, on the other hand, $N(a'|z'\rangle - a''|z''\rangle)$ *differs* from $\pm|z\rangle$, and a continuity argument is necessary for the final choice.

For the proof, figures, and many finer details, in particular regarding the sign ambiguity, we must refer to Ref. 5, Chap. 1.6. (To make the comparison, it is necessary to observe that the structure considered there corresponds to considering $\mathbf{C}^2$ and the *bi*linear form $\{\cdot|\cdot\}$ alone, while our "*sequi*linear" scalar product $\langle\cdot|\cdot\rangle$ corresponds, in the framework of that book, to singling out a timelike future-directed unit four-vector, whose orthogonal space is the $\mathbf{R}^3$ used here.)

The purpose of indicating these constructions here was just to point out how many intricate geometric features are hidden in the algebraically deceptively simple framework of complex Hilbert space for quantum mechanics in a case where they still *can* be visualized. This is in marked contrast to the real vector calculus used to describe geometry and classical mechanics in Euclidean $\mathbf{R}^3$!

We conclude this section with a topological remark: The Hopf fibering of $\mathbf{S}^3$ is "nontrivial," i.e., there is no bijection, continuous in both directions, between $\mathbf{S}^3$ and $\mathbf{S}^2 \times \mathbf{S}^1$ (the latter is not simply connected, containing noncontractible loops, while the former is). This has the consequence that it is not possible to choose phase factors for all (pure) states of the system that would vary continuously over *all* state space. In the $\mathbf{S}^2$ picture, this appears as the impossibility to find a continuous field of unit tangent vectors all over the sphere $\mathbf{S}^2$, a fact that is known as the "impossibility to comb a hedgehog."

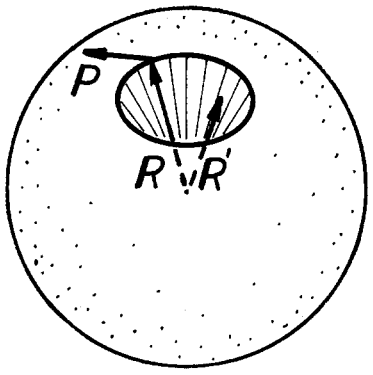

Fig. 4. States and normalized state vectors on the unit ball. Mixed states correspond to interior points (e.g., $\mathbf{R}'$), pure states to surface points (e.g., $\mathbf{R}$), and normalized state vectors to unit tangent at surface points (e.g., $\mathbf{P}$). Phase changes in state vectors rotate these tangents about their point of contact by twice the phase angle increment.

IV. TIME EVOLUTION AND ADIABATIC CHANGES

We now consider the appearance of quantum mechanical time evolution in our geometric representation of states and state vectors. Generally, it is given in the Schrödinger

picture by the Schrödinger equation for state vectors

$$\frac{d}{dt}|z(t)\rangle = -\frac{i}{\hbar}H|z(t)\rangle \tag{32}$$

or the Bloch equation for density matrices

$$\frac{d}{dt}\rho(t) = -\frac{i}{\hbar}[H,\rho(t)], \tag{33}$$

where H, the Hamiltonian, is a Hermitian operator. For two-level systems, H is a Hermitian 2×2 matrix which we may write, similar to (6), as

$$\begin{pmatrix} H_{11} & H_{12} \\ H_{21} & H_{22} \end{pmatrix} = H = H_0\mathbf{1} + \mathbf{H}\cdot\boldsymbol{\sigma}, \tag{34}$$

where $H_{12} = \overline{H}_{21}$ is complex while $H_{11}, H_{22}, H_0, \mathbf{H}$ are real. Frequent use will be made of the relation

$$(\boldsymbol{\alpha}\cdot\boldsymbol{\sigma})(\mathbf{b}\cdot\boldsymbol{\sigma}) \equiv \mathbf{a}\cdot\mathbf{b}\mathbf{1} + i(\mathbf{a}\times\mathbf{b})\cdot\boldsymbol{\sigma}, \tag{35}$$

which characterizes the algebra of the Pauli matrices. They lead from (33), (6), and (34) directly to

$$\frac{d\mathbf{R}}{dt} = \dot{\mathbf{R}} = \frac{2}{\hbar}\mathbf{H}\times\mathbf{R}, \tag{36}$$

describing time evolution in the $\mathbf{S}^2 \subset \mathbf{R}^3$ picture. It follows that $\frac{1}{2}(\mathbf{R}^2) = \mathbf{R}\cdot\dot{\mathbf{R}} = 0$: A pure state will remain pure, a mixed state will remain mixed. (This follows quite generally from the Hermiticity of H, i.e., the unitary nature of time evolution.)

The geometrical interpretation of (36) is that $\mathbf{R}(t)$ at each instant of time undergoes an infinitesimal rotation around the axis given by $\mathbf{H}(t)$, with angular velocity $2|\mathbf{H}|/\hbar$. So if H is time independent, this will just be a rigid rotation, or precession, of $\mathbf{R}(t)$ around $\mathbf{H}$, as exemplified by the precession of a spin-1/2 in a constant magnetic field [Fig. 5(a)].

However, if $H(t)$ depends on time, the orbit of $\mathbf{R}(t)$ depends very much on the ratio of the angular velocity $2|\mathbf{H}|/\hbar$ to the rate of change of $H(t)$. To discuss this, first note that the eigenvalues and eigenstates of H are given by

$$E = H_0 \pm |\mathbf{H}|, \quad \rho_E = \tfrac{1}{2}(\mathbf{1} + \mathbf{R}_E\cdot\boldsymbol{\sigma}),$$
$$\mathbf{R}_E = \pm\mathbf{H}/|\mathbf{H}|. \tag{37}$$

[Verify $H\rho_E = E\rho_E$ using (35); since $\rho_E = |E\rangle\langle E|$ where $|E\rangle$ is a corresponding eigenvector, this is equivalent to $H|E\rangle = E|E\rangle$.] If H is time independent, $\mathbf{R} = \mathbf{R}_E$ solves (36) and is a stationary state: The precession circle degenerates into a fixed point (the two possibilities $\pm$ are antipodal, corresponding to the orthogonality of eigenvectors). If H depends on time, $E = E(t)$ and $\mathbf{R}_{E(t)}$ depend on time; they are called instantaneous eigenvalues and eigenstates, respectively, and $\mathbf{R}_{E(t)}$ is *not* a solution of (36). We may now characterize the rate of change of $H(t)$ by the velocity of $\mathbf{R}_{E(t)}$, which actually is an angular velocity since $\mathbf{R}_{E(t)}$ moves over the unit sphere. Its order of magnitude is $|\dot{\mathbf{H}}|/|\mathbf{H}|$; and we can now get a qualitative picture of $\mathbf{R}(t)$ in the so-called *adiabatic limit* $2|\mathbf{H}|/\hbar \gg |\dot{\mathbf{H}}|/|\mathbf{H}|$. Then $\mathbf{R}(t)$ describes fast circles around the center $\mathbf{R}_{E(t)}$ which get slowly displaced at the same time [Fig. 5(b)] (see Ref. 1, p. 10–17).

An interesting special case arises if at time $t = 0$, say, we require $\mathbf{R}(0) = \mathbf{R}_{E(0)}$. Then, from our qualitative picture, $\mathbf{R}(t)$ must coincide with $\mathbf{R}_{E(t)}$ in the adiabatic limit. This can be made into a precise general theorem (the *adiabatic theorem*[6]). It has been of recent interest in this special case

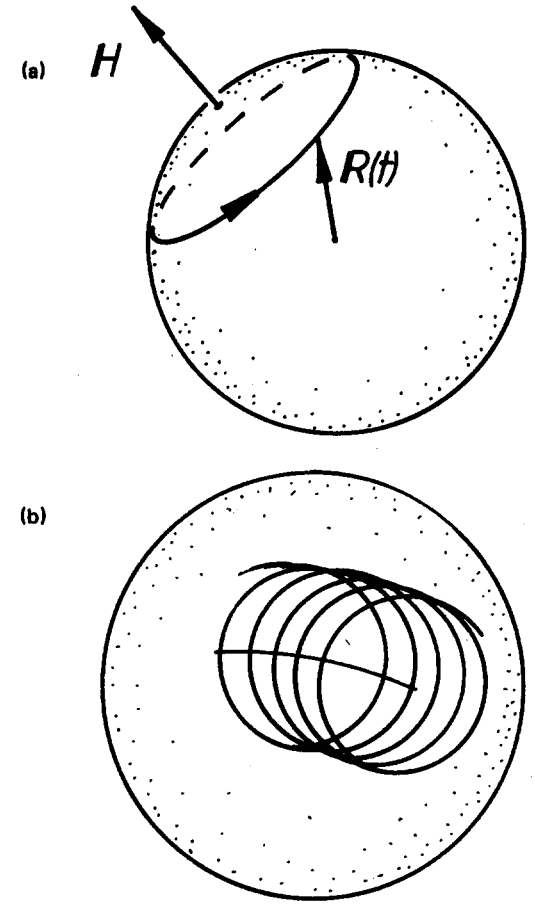

Fig. 5. (a) Time evolution for time-independent Hamiltonian. $\mathbf{R}(t)$ precesses around the axis $\mathbf{H}$. (b) Time evolution in the adiabatic limit. $\mathbf{R}(t)$ spirals around the "soul" $\mathbf{R}_{E(t)}$.

to ask for the time evolution of the *phase* of the *state vector*, the point here being the following.

In the time-independent case, if initially $\mathbf{R}(0) = \mathbf{R}_E$, then $\mathbf{R}(t) = \mathbf{R}_E$, so $|z(t)\rangle$ differs from $|z(0)\rangle$ by phase only, in fact, $|z(t)\rangle = \exp(-iEt/\hbar)|z(0)\rangle$. In the $\mathbf{S}^2$ picture, the unit tangent $\mathbf{P}(t)$ representing the phase of $|z(t)\rangle$ rotates in the tangent plane at $\mathbf{R}_E$ with angular frequency $2E/\hbar$. Assume now there is adiabatic time variability such that after time T we have $\mathbf{H}(T)/|\mathbf{H}(T)| = \mathbf{H}(0)/|\mathbf{H}(0)|$. Then if $\mathbf{R}(0) = \mathbf{R}_{E(0)}$, in the adiabatic limit $\mathbf{R}(t) \approx \mathbf{R}_{E(t)}$ traces a *closed curve* on $\mathbf{S}^2$: $\mathbf{R}(T) \approx \mathbf{R}_{E(T)} = \mathbf{R}_{E(0)} = \mathbf{R}(0)$. From the stationary situation just mentioned, one would guess that the phase increments picked up by $|z(t)\rangle$ during the round trip $\mathbf{R}(t)$ would add up just to

$$|z(T)\rangle = \exp\left(-\frac{i}{\hbar}\int_0^T E(t')dt'\right)|z(0)\rangle.$$

But this is *not* the case, i.e., the ("dynamical phase" split off) redefined state vector

$$|z'(t)\rangle := \exp\left(\frac{i}{\hbar}\int_0^t E(t')dt'\right)|z(t)\rangle \tag{38}$$

does not, in the adiabatic limit, have $|z'_{\text{ad}}(T)\rangle = |z'_{\text{ad}}(0)\rangle = |z(0)\rangle$, but instead changes phase such as to satisfy

$$\langle z'_{\text{ad}}(t)|\dot{z}'_{\text{ad}}(t)\rangle = 0. \tag{39}$$

We shall not give a proof of this general result (which is

included as a technical means in all proofs of the adiabatic theorem, a "convenient" phase gauge, first invented by Fock[7] and characterized by him in terms of a "minimum oscillation principle"), obtained by making sense of $\infty \cdot 0$ by a simple observation.[8] Rather, we want to illustrate it in our $\mathbf{S}^2$ picture. Corresponding to the phase redefinition (38), we have a redefined $\mathbf{Z}'(t) = \mathbf{P}'(t) + i\mathbf{Q}'(t)$ for $|z'(t)\rangle$, and we now consider the adiabatic limit thereof. From $\bar{z}_1\dot{z}_1 + \bar{z}_2\dot{z}_2 = 0$ we conclude the existence of some complex function $\lambda(t)$ such that

$$\dot{z}_1 = -\lambda\bar{z}_2, \quad \dot{z}_2 = \lambda\bar{z}_1. \tag{40}$$

Going back to the definition of $\mathbf{Z}$, differentiating and inserting (40) we obtain

$$\dot{\mathbf{Z}} = -2\lambda\,\mathbf{R}. \tag{41}$$

Therefore, $\mathbf{Z}'_{\text{ad}}$ must satisfy

$$\mathbf{R}_E \times \dot{\mathbf{Z}}'_{\text{ad}} = 0, \quad \text{i.e.,} \quad \mathbf{R}_E \times \dot{\mathbf{P}}'_{\text{ad}} = 0 = \mathbf{R}_E \times \dot{\mathbf{Q}}'_{\text{ad}}. \tag{42}$$

Thus, while a similar calculation using the definition of $\mathbf{R}$ results in

$$\dot{\mathbf{R}}_E = \bar{\lambda}\,\mathbf{Z}'_{\text{ad}} + \lambda\,\mathbf{Z}'_{\text{ad}}, \tag{43}$$

which is no new condition since it just says $\mathbf{R}_E \cdot \dot{\mathbf{R}}_E = 0$ or $\mathbf{R}_E^2 = \text{const} = 1$ (already known), (42) is a genuine condition on $\mathbf{Z}'_{\text{ad}}$ or $\mathbf{P}'_{\text{ad}}$. (In $|z\rangle$ language: preservation of normalization requires $0 = \langle z|z\rangle = \langle \dot{z}|z\rangle + \langle z|\dot{z}\rangle = 2\,\text{Re}\langle z|\dot{z}\rangle$, a weaker condition than $\langle z|\dot{z}\rangle = 0$.) Its geometric meaning[9] in the $\mathbf{S}^2$ picture is the following: Proceed in infinitesimal steps to obtain $\mathbf{Z}'_{\text{ad}}(t + \Delta t)$ at $\mathbf{R}_E(t + \Delta t)$ from $\mathbf{Z}'_{\text{ad}}(t)$ at $\mathbf{R}_E(t)$ by first attaching $\mathbf{Z}'_{\text{ad}}(t)$ at $\mathbf{R}_E(t + \Delta t)$ (Euclidean parallel shift in $\mathbf{R}^3 \supset \mathbf{S}^2$)—it now "sticks out" of the sphere—and then projecting back to the tangent plane along $\mathbf{R}_E(t + \Delta t)$). Indeed, writing this out to order Δt yields

$$\dot{\mathbf{Z}}'_{\text{ad}} = -(\mathbf{Z}'_{\text{ad}} \cdot \mathbf{R}_E)\mathbf{R}_E, \tag{44}$$

and this is of the form (41) and is, via $(\mathbf{R}_E \cdot \mathbf{Z}'_{\text{ad}})^{\cdot} \equiv 0$, implied by (41).

The prescription just given is nothing but the well-known Levi-Civita "geodesic parallel transport" of tangents to a surface, embedded in Euclidean space, along a given curve. It plays a considerable role in Riemannian differential geometry, and has also been given a classical mechanics interpretation by Radon,[10] again involving an adiabatic limit.

What is remarkable about this transport is that it is path dependent, or equivalently, it does not lead back to the starting value $\mathbf{Z}'_{\text{ad}}(0) = \mathbf{Z}(0)$ when executed along the round trip $\mathbf{R}_{\text{ad}}(t) = \mathbf{R}_{E(t)}$, $0 \leqslant t \leqslant T$, considered before. Rather, $\mathbf{P}'_{ad}(T)$ is obtained from $\mathbf{P}'(0)$ by rotating it through a certain angle, called a *holonomy* transformation. Books on differential geometry[11] inform us that this angle between $\mathbf{P}'_{\text{ad}}(0)$ and $\mathbf{P}'_{\text{ad}}(T)$ will be given—as an easy consequence of the Gauss–Bonnet theorem—by the surface integral of the Gaussian curvature of the surface over the domain encircled by the round trip (if the latter is smooth), i.e., in the case of the unit sphere $\mathbf{S}^2$, simply by the surface area encircled. The corresponding phase between $|z'_{\text{ad}}(0)\rangle$ and $|z'_{\text{ad}}(T)\rangle$ is a very special case of what is known as the *Berry phase*.[12,8] What is remarkable here is that it depends on $H(t)$ only through $\mathbf{H}(t)/|\mathbf{H}(t)|$, which is sometimes described as a kind of *universality*.

To finish up, let us also have a look on adiabatic phase transport in the $\mathbf{R}^4 \supset \mathbf{S}^3$ and stereographic $\mathbf{R}^3$ picture. Writing out $\langle z|\dot{z}\rangle = 0$ in this formalism and looking at the imaginary part, we get

$$X_1\dot{X}_2 - X_2\dot{X}_1 + X_3\dot{X}_4 - X_4\dot{X}_3 = 0.$$

This equation says that $\dot{X}$ is, in $\mathbf{R}^4$, not only orthogonal to X (thus tangent to $\mathbf{S}^3$ as it should) but orthogonal to the Hopf fiber passing through X, whose tangent there is JX [see (13)]. Since stereographic projection preserves angles, this property holds also in the stereographic $\mathbf{R}^3$ picture. To $|z'_{\text{ad}}(t)\rangle$ there corresponds, then, a curve in $\mathbf{S}^3$ or stereographic $\mathbf{R}^3$, lying on a tubular closed surface formed by a one-parameter family of phase circles; the curve is an orthogonal trajectory of these circles and does *not* return to its starting point when it hits the starting circle again. (For example, if $\mathbf{R}_{E(t)}$ is a circle $\vartheta = \text{const}$ in the $\mathbf{S}^2$ picture, then from Sec. III we know that the tubular surface is just a torus in the stereographic $\mathbf{R}^3$ picture, with one family of Villarceau circles on it.) This kind of picture is, however, less directly related to a Gaussian curvature integral in the elementary sense, but requires fiber bundle concepts as does the general case considered in Refs. 8 and 12.

V. CONCLUDING REMARK

In this article, we have put some more or less well-known facts about states and state vectors of two-level systems—some old and some new ones—into perspective, thus illuminating the geometrical structures involved in the complex Hilbert space description. We must hurry to emphasize that another "geometrical" aspect of quantum mechanics was totally omitted here, the one concerning observables. It is generally true that the set of states and its structures is determined by the set of observables which generate, over $\mathbf{C}$, a certain associative, but not necessarily commutative, algebra (in our two-level example, the algebra generated, e.g., by σ_1, σ_2). It seems that such algebras have their own, noncommutative, geometry—but that is a very different and very abstract story beyond the scope of this article.

What should also be pointed out is the fact that the structure of the state space of N-level quantum systems is much more complicated for $N > 2$ than it is for $N = 2$. For example, for $N = 2$, the set of extremal points (pure states) is identical with the topological boundary of the (convex) domain of positivity within the set of all Hermitian $N \times N$ matrices of unit trace. For $N > 2$, this cannot be the case already for reasons of dimension, and this boundary has, in fact, quite interesting geometrical properties, involving curved edges and rulings of various dimensions, etc. and a general kind of "obliqueness" (stemming from the fact that the unitary group $\mathbf{U}(N)$ of $\mathbf{C}^N$ is, by its action on density matrices, homomorphically mapped only onto a genuine subgroup of the group $\mathbf{SO}(N^2 - 1, \mathbf{R})$ of rotations in state space). Also, for $N > 2$ there is the possibility of nontrivial Hamiltonians with degenerate eigenvalues, leaving room for additional phenomena. We cannot follow this here.

ACKNOWLEDGMENTS

I have profited from conversations with D. Grau, H. Grosse, R. Penrose, and A. Uhlmann, and I am indebted to R. Penrose for his kind permission to reproduce his "twistor figure" as Fig. 1.

[1] R. P. Feynman, R. B. Leighton, and M. Sands, *The Feynman Lectures on Physics* (Addison-Wesley, Reading, MA, 1965), Vol. 3; see Secs. 9,

10, and 11 for two-level systems.

[2] L. I. Schiff, *Quantum Mechanics* (McGraw-Hill, New York, 1968), 3rd ed. The relevant parts here are Secs. 23, 24, and 42, and, for adiabatic changes of state, Sec. 35.

[3] M. Berger, *Geometry* (Springer-Verlag, Berlin, 1987), Vol. I. Sec. 10.12; Vol. II, Secs. 18.8 and 18.9. Figure 1 is taken from p. 62 of R. Penrose and W. Rindler, *Spinors and Space-Time. Vol. 2: Spinor and Twistor Methods in Space-Time Geometry* (Cambridge U.P., New York, 1986); versions of it appear in several other articles by R. Penrose on twistor theory. We recommend to the reader his essay "The Geometry of the World," in *Mathematics Today*, edited by L. A. Steen (Springer-Verlag, New York, 1978), pp. 83–124. In fact, the present subsection could be taken as a partial elaboration of his remarks in the very last paragraph of his essay. We also point out here that the Hopf fibering appears, in theoretical physics, in still a third context—the Dirac magnetic monopole of lowest nontrivial charge; see A. Trautman, "Solutions of the Maxwell and Yang–Mills equations associated with Hopf fibrings," Int. J. Theor. Phys. **16**, 561–565 (1977).

[4] H. Weyl, *The Theory of Groups and Quantum Mechanics* (Dover, New York, 1950), pp. 144–145.

[5] R. Penrose and W. Rindler, *Spinors and Space-Time, Vol. 1: Two-Spinor Calculus and Relativistic Fields* (Cambridge U.P., New York, 1984), Secs. 1.4 and 1.6.

[6] M. Born and V. A. Fock, "Beweis des Adiabatensatzes," Z. Phys. **51**, 165–180 (1928); T. Kato, "On the adiabatic theorem of quantum mechanics," J. Phys. Soc. Jpn. **5**, 435–439 (1950); A. Messiah, *Quantum Mechanics* (North-Holland, Amsterdam, 1962), Vol. II, pp. 744–754.

[7] V. A. Fock, "Ueber die Beziehung zwischen den Integralen der quantenmechanischen Bewegungsgleichungen und der Schrödingerschen Wellengleichung," Z. Phys. **49**, 323–338 (1928), Appendix.

[8] B. Simon, "Holonomy, the quantum adiabatic theorem, and Berry's phase," Phys. Rev. Lett. **51**, 2167–2170 (1983).

[9] J. Anandan and L. Stodolsky, "Some geometrical considerations on Berry's phase," Phys. Rev. D **35**, 2597–2599 (1987). For illustration and the appearance of this transport process in a rather different physical situation, see H. K. Urbantke, "Physical holonomy, Thomas precession, and Clifford algebra," Am. J. Phys. **58**, 747–750 (1990).

[10] J. Radon, "Mechanische Herleitung des Parallelismus von T. Levi Civita, *Collected Works* (edited by P. Gruber *et al.*, Birkhäuser-Verlag, Basel, 1987), Vol. 2, pp. 354–369. This work is identical to his contribution, on pp. 331–346, to F. Klein, "Vorlesungen über höhere Geometrie," edited by W. Blaschke (Springer-Verlag, Berlin, 1926). The related work by M. Kugler and S. Shtrikman, "Berry's phase, locally inertial frames, and classical analogue," Phys. Rev. D **37**, 934–937 (1988), is the basis of the device shown on p. 27 of the essay M. V. Berry, "The geometric phase," Sci. Am. **259**(6), 26–32 (1988). The Foucault pendulum example mentioned in all these articles is also discussed by H. Freudenthal, "Foucaults Pendelversuch in der Differentialgeometrie," Math. Phys. Semesterber. **5**, 230–238 (1957) and, more recently, by J. B. Hart, R. E. Miller, and R. L. Mills, "A simple geometric model for visualizing the motion of a Foucault pendulum," Am. J. Phys. **55**, 67–70 (1987).

[11] K. Strubecker, *Differentialgeometrie* (Walter de Gruyter Verlag, Berlin, 1969), Vol. III, Secs. IV.23, Satz 1. Vol. II of this work gives, in Sect. III.40, a few geometric constructions for parallel transport on two-surfaces embedded in Euclidean three-space. See also J. Radon, Ref. 10, p. 366.

[12] M. V. Berry, "Quantal phase factors accompanying adiabatic changes," Proc. R. Soc. London. Ser. A **392**, 45–57 (1984); with spin-1/2, the effect was experimentally demonstrated in T. Bitter and D. Dubbers, "Manifestation of Berry's topological phase in neutron spin rotation," Phys. Rev. Lett. **59**, 251–254 (1987); D. Dubbers, "Measurement of the Berry phase with polarized neutrons," Physica B **151**, 93–95 (1988).

Improved numerical solutions of Laplace's equation

Philip W. Gash
Physics Department, California State University, Chico, California 95929-0202

(Received 20 June 1990; accepted for publication 10 September 1990)

Three different methods for generating numerical solutions of Laplace's equation are derived using a differential operator formalism for a Taylor series expansion of the electric potential about a point. The expansions are evaluated on three different two-dimensional grids in the x-y plane to yield algorithms good up to, but not including, fourth order. The accuracy and convergence of the algorithms are compared by applying them to a rectangular boundary value problem. Second, it is shown that the convergence criterion for numerical solutions can be interpreted as a charge density; and, therefore, the numerical solutions are, in fact, solutions of Poisson's equation. Further, it is demonstrated that the numerical solutions of Laplace's equation are bounded above and below by the solutions of Poisson's equation corresponding to a maximum uniform charge density derived from the convergence criterion. For this reason, it is recommended that numerical solutions of Laplace's equation should be accompanied by a statement of the maximum uniform charge density.

I. INTRODUCTION

In recent years the accessibility of personal computers and spreadsheet programs has awakened both pedagogical and practical interest in numerical solutions to physics problems.[1–5] In general, these treatments start from a finite-difference algorithm that approximates the differential equation that describes the physical process in question. Next, the treatments discuss how a particular algorithm works, and then they ask the student to solve a few problems with it. An important secondary question about the algorithm, which is not often addressed, is "How good is the solution?" In more specific terms, what about its accuracy—how close is the numerical solution to the analytical solution? An what about its rate of convergence—will it yield a solution quickly, or are hundreds of

